# Finite element simulation and experimental analysis of thermal distribution of optical transceiver

**ZHANG Sheng[1, a], NIE Lei[2, b*], JIANG Chuan Kai[3, c]**

School of Mechanical Engineering ,Hubei Univ. of Tech. ,Wuhan 430068, China

[a]zhang_sheng9311@163.com

**Abstract.** In order to optimize the heat dissipation design, the finite element simulation and temperature measurement experiment were used to research the optical transceiver temperature distribution. The results indicated that the shield cage impaired the convective heat transfer efficiency of the photoelectric conversion chip in the optical transceiver. Thus the heat dissipation of the device was weakened. The optimization method was put forward to introduce the external ducts by improving the structure design of the shield cage. The simulation showed the effectiveness of this method which could improve the heat dissipation efficiency of optical transceiver products.

## 1. Introduction

With the development of optical communication industry which tended toward the miniaturization and integration , the energy density of optical transceiver, which was a typical optical communication device, was getting higher and higher. Heat dissipation now was being a severe challenge for these transceivers and having received great attention from research institutions and industries. Cai proposed two methods to enhance the cooling efficiency of the optical module. One was to open some holes on the PCB board, the other was to fill a thin layer of electric-insulated heat-conducted material between the PCB and package [1-2].And artificial diamonds with high thermal conductivity were embedded in the PCB of the high power devices of optical module, which reduced the difference of temperature between heating part and module shell and achieved better cooling efficiency [3].

These research above provided useful enlightment for the thermal design of optoelectronic devices represented by optical transceivers. However, it was difficult to obtain the internal temperature information directly because the heating device was enclosed inside the packaging. The prototype of optical transceiver products were chose for the research. The simulation was carried out to reveal the internal temperature distribution, found the temperature concentrated area and the route of heat dissipation. After that, the infrared measurement experiment was presented to verify the accuracy of the simulation results and mastered the main form of heat transfer. Finally, based on the conclusion, the optimization measures were put forward.

## 2. Finite element analysis principle

There were three kinds of heat transfer: radiation, convection and conduction. The heat conduction equation described the internal temperature distribution of the structure. Differential equations could be simplified as follows：

$$pc\frac{\partial T}{\partial t}=\frac{\partial}{\partial x}\left(\lambda_x\frac{\partial T}{\partial x}\right)+\frac{\partial}{\partial y}\left(\lambda_y\frac{\partial T}{\partial y}\right)+\frac{\partial}{\partial z}\left(\lambda_z\frac{\partial T}{\partial z}\right)+\rho q_i\,. \tag{1}$$

Among, p was the material density, c was material specific heat capacity, λx, λy, λz was the heat transfer coefficient x, y, z indirection, qi was the internal chip density, t is time.

The left side of the differential equation represented the amount of heat required per unit time. The first, second and third items on the right side described the heat transfer to the material along the x, y, z three directions per unit time. The last item on the right side was the amount of heat generated of heat source per unit time.

In this paper, the temperature field was isotropic, and the differential equation could be simplified as follows:

$$\frac{\partial^2 T}{\partial x^2}+\frac{\partial^2 T}{\partial y^2}+\frac{\partial^2 T}{\partial z^2}+\frac{\rho q_i}{\lambda}=0\,. \tag{2}$$

The purpose of the study was to find the boundary value of the differential equation. The boundary value studied was a mixed problem of the value of the boundary temperature and the heat transfer between the boundary and the surrounding medium, its mathematical expression was:

$$\lambda\left(\frac{\partial T}{\partial n}\right)_\tau+\alpha(T-T_m)-q_0=0\,. \tag{3}$$

Among, α was heat transfer coefficient; Tm was surrounding medium temperature.

## 3. Finite simulation analysis

*3.1. Design of simulation analysis.*

The structure of optical transceiver generally consisted of six parts: the upper and lower shell, the internal structure, the shield cage, the photoelectric conversion chip and the PCB as shown on Fig. 1. The photoelectric conversion chip was packaged on the PCB. The shield cage was used to provide electromagnetic isolation, which was tightly bonded with the PCB by thermosetting polymer. In order to investigate the influence of shield cage on heat dissipation and temperature distribution, two different models were created: with shield cage and without shield cage.

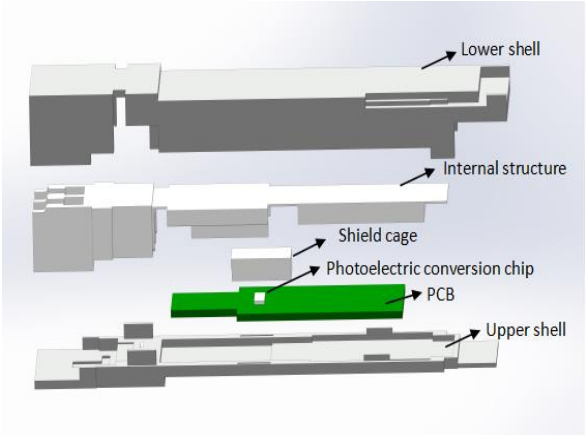


**Figure. 1** 3D model of the optical transceiver

The power of photoelectric conversion chip was 1W, and the ambient temperature was set to 25 ℃. The different material of characteristic parameters were listed in Table 1, such as Young's modulus, thermal conductivity and electrical conductivity.

**Table 1** Simulation parameters

| Property | Thermal conductivity [W/m.K] | Electrical conductivity [Ω.m] | Young's modulus [N/m$^2$] | Poisson's ratio |
|---|---|---|---|---|
| Upper and lower shell, internal structure | 237 | 2.33E-08 | 70E+09 | 0.30 |
| Shield cage | 214 | 2.83E-08 | 70E+09 | 0.32 |
| Photoelectric conversion chip | 15 | 1.18E-06 | | |
| PCB | 6.5 | 1.2E+12 | | |

*3.2. Simulation results analysis.*

Fig. 2 showed the temperature distribution of the device without shield cage. The chip temperature was the maximum, about 50.8℃. The upper shell surface temperature was about 33.5℃, because of natural convection. Fig. 3 was the cross-sectional temperature distribution of the device. The PCB was in separated state with the load-carrying component, because the intercept plane did not contain support points. The temperature was concentrated on the front of the PCB board, which was gradually decreased from the chip to the middle of PCB and approximately tended to be the same at the end of PCB.

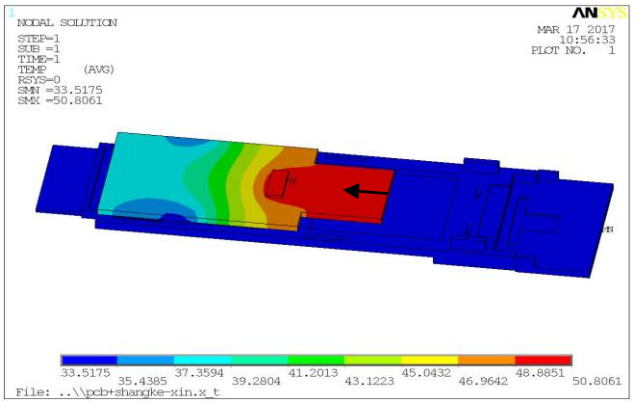


**Figure. 2** Temperature distribution without shield cage

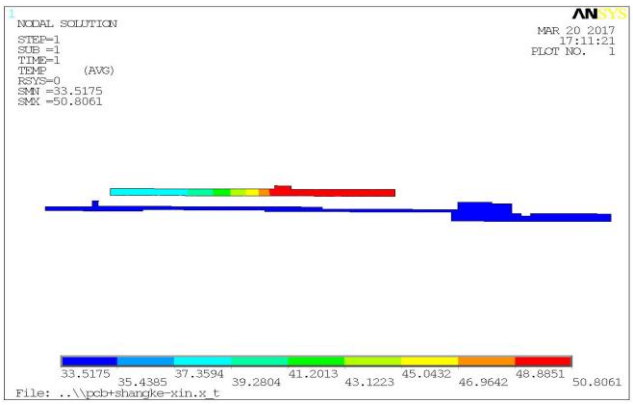


**Figure. 3** Device section temperature distribution

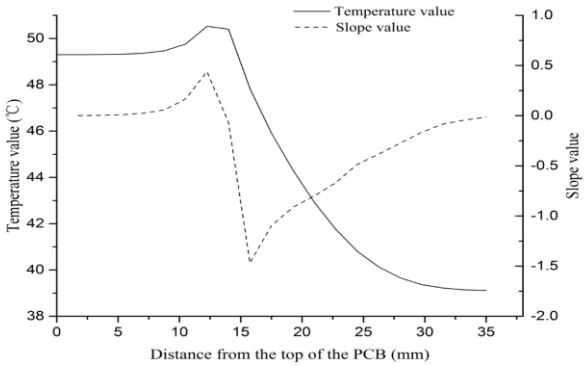


**Figure. 4** PCB board temperature distribution

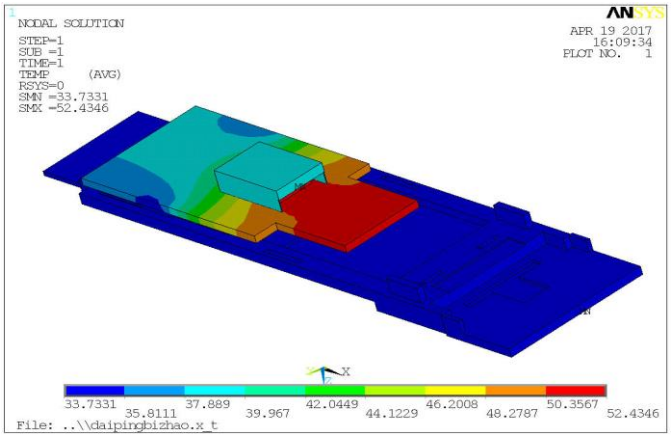


**Figure. 5** Temperature distribution with shield cage and slope value

When the PCB board temperature distribution and slope value (the direction of the arrow in Fig. 2) were compared in Fig. 4, it could be found that the slope of the temperature curve of PCB board was almost straight and the position near the chip was a high temperature area and slope value gradually reached its peak value. With the distance increased, the temperature dropped sharply, and the rate of temperature change gradually became slow after the valley value was reached.

The temperature distribution of the device with shield cage was generally similar to Fig. 2 (as shown in Fig. 5). But the maximum temperature of the chip was about 52.4℃, which was 1.6℃ higher than that without shield cage. The shield cage temperature was 37℃, and obviously lower than the temperature of PCB. It indicated that the temperature of the PCB board was not effectively transferred to the shield cage. The shield cage hindered the heat dissipation of the chip and increased the temperature.

*3.3. Temperature measurement.*

A test system was built to verify the validity of the simulation analysis, as shown in Fig. 6. The optical transceiver was placed on the platform, and the infrared imager was mounted on a tripod to record the surface temperature distribution of the device.

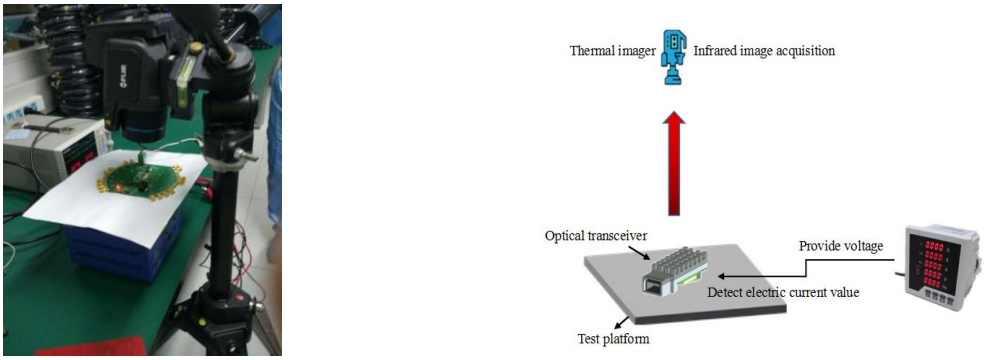


(a) (b)

**Figure. 6** Temperature measuring system. (a)Test physical picture, (b) Test sketch picture

From Fig. 7, the temperature distribution without shield cage could be obtained clearly. The brightest area meant the highest temperature, i.e. the photoelectric conversion chip. The brightness at the front of chip indicated the temperature concentrated on this part, and gradually reduced from the front to the end of device. The results were similar to those of Fig. 2.

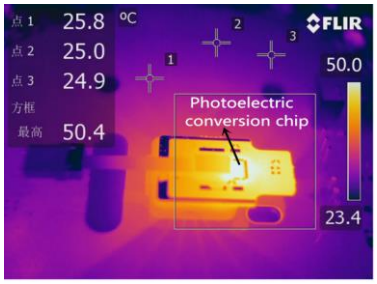


**Figure. 7** Infrared temperature distribution image without shield cage

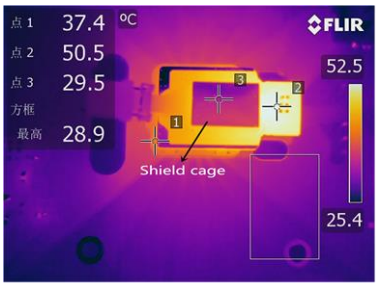


**Figure. 8** Infrared temperature distribution image with shield cage

Fig. 8 showed the temperature distribution with shield cage. The highest temperature on the temperature bar approximately represented the chip temperature which couldn't be directly measured due to the presence of the shield cage, it was 52.5℃. The temperature of the shield cage in point 3 was 29.5℃ and 20℃ lower than that of the chip. The results were similar to those of Fig. 5.

## 4. Improvement measure

The external air duct was brought to enhance the convection of the chip by alternately punching on the side of the shield cage (as shown in Fig. 9).

**Figure. 9** The improvement shield cage model

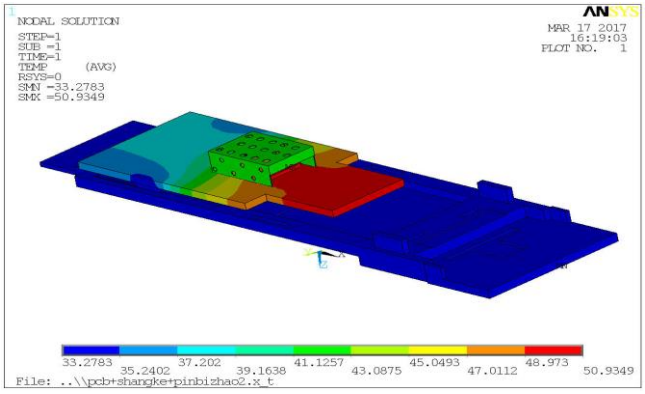


**Figure. 10** Simulation of thermal distribution of improvement optical transceiver

Fig. 10 showed the simulation results of the improved optical transceiver. Compared with Fig. 5, the temperature of the chip was decreased nearly 1.4℃, which indicated that the measure was effective after the introduction of the external air duct.

## 5. Result analysis

The simulation results were credible because the simulative temperature distribution was accordant with the measurement result. Thus conclusions could be drawn as follow.

The temperature distribution was revealed. The temperature of the photoelectric conversion chip was the highest all over the device. And the temperature gradient reached the peak at the middle of the PCB. The temperature of the edge area of PCB near photoelectric conversion chip was almost same with that of the chip and the far-end of PCB was relatively cool and had the same temperature with the outside shell due to the sufficient convection.

The shield cage hindered the heat dissipation of the chip. As a result, the temperature of the chip with shield cage was 2.8℃ higher than that without shield cage. It was obvious that the chip were enclosed by shield cage in the shell where the air convection efficiency was very low.

The heat dissipation of heat conduction was inefficient. The contact areas between chip and other parts were so small that the heat generated in the packaging of device couldn't effectively be conducted to the outside.

## 6. Conclusion

The finite element simulation and temperature measurement had been carried out to reveal the temperature distribution of the optical transceiver. It was found that the existence of the shield cage results in low convective heat transfer, and the temperature was easy to accumulate in the chip. The modified shield cage with additional through holes was proposed and the simulative result proved that it could reduce the temperature to a certain extent.

**Acknowledgement**
This work was funded by the Key Project of Educational Commission of Hubei Province of China (D20131407), open Foundation of State Key Lab of Digital Manufacturing Equipment & Technology (DMETKF2014017) and Special Fund in the Public interest of General Administration of Quality Supervision Inspection and Quarantine of P.R.China (201310004).

**References**

[1] Cai Y Y. The electromagnetic interference shielding and thermal design for high-speed broadband optical module [D]. Southeast University, 2016.
[2] Haghighi E B, Phan T L, Wuttijumnong V, et al. Improved Air Cooling Heat Pipe Based Thermal Solutions for Heat Sinks in Optical Plug Modules[C]// ASME 2015 International Technical Conference and Exhibition on Packaging and Integration of Electronic and Photonic Microsystems Collocated with the ASME 2015, International Conference on Nanochannels, Microchannels, and Minichannels. 2015:V001T09A007.
[3] Li W Q, Wang X F, Ling X, Li X T. The Thermal Structure of The Optical Module [P]. Fu Jian：CN205301638U, 2016-06-08.
[4] Lu J F, Sun F. Heat Radiation Design and Simulation of a Module [J]. Electronic Sci. &Tech, 2013, (08):19-21
[5] Huang S L, Liu Z M, Zhai L Q. Optical Module Cooling Structure and Electronic Products[P]. GuangDong:CN104661487A, 2015-05-27.
[6] Baek Y, Han Y T, Lee C W, et al. Optical components for 100G ethernet transceivers[C]// Opto-Electronics and Communications Conference. IEEE, 2012:218-219.
[7] Zhong D, Yang S, Li S, et al. METHOD AND DEVICE FOR OPTICAL POWER CONTROL: EP 2713528 A1 [P]. 2014.
[8] Cho H, Kapur P, Saraswat K C. Power Comparison Between High-Speed Electrical and Optical Interconnects for Interchip Communication[J]. Lightwave Technology Journal of, 2004, 22(9):2021-2033.
[9] Ke K. Design and Realization of 100Gbit/s CFP Optical Transceiver Module [D]. Fiber Home Technologies Group, 2015.
[10] Shahbaz M, Lean H H, Shabbir M S. High-speed PCB signal integrity analysis based on digital circuit system[J]. Journal of Guilin University of Electronic Technology, 2012, 16(5):2947-2953.